Liu et al. Nanoscale Research Letters (2018) 13:405
https://doi.org/10.1186/s11671-018-2825-6

Nanoscale Research Letters

NANO EXPRESS Open Access

Investigation of the Energy Band at the Molybdenum Disulfide and ZrO_2 Heterojunctions

Xinke Liu[1*], Cong Hu[1], Kuilong Li[2*], Wenjia Wang[2], Zhiwen Li[1], Jinping Ao[1], Jing Wu[3], Wei He[4], Wei Mao[5], Qiang Liu[6], Wenjie Yu[6] and Ren-Jei Chung[7]

Abstract

The energy band alignment at the multilayer-MoS_2/ZrO_2 interface and the effects of CHF_3 plasma treatment on the band offset were explored using x-ray photoelectron spectroscopy. The valence band offset (VBO) and conduction band offset (CBO) for the MoS_2 /ZrO_2 sample is about 1.87 eV and 2.49 eV, respectively. While the VBO was enlarged by about 0.75 eV for the sample with CHF_3 plasma treatment, which is attributed to the up-shift of Zr 3d core level. The calculation results demonstrated that F atoms have strong interactions with Zr atoms, and the valence band energy shift for the d-orbital of Zr atoms is about 0.76 eV, in consistent with the experimental result. This interesting finding encourages the application of ZrO_2 as gate materials in MoS_2-based electronic devices and provides a promising way to adjust the band alignment.

Keywords: Energy band alignment, X-ray photoelectron spectroscopy, MoS_2/ZrO_2, CHF_3 treatment

Introduction

In the past decades, SiO_2/Si-based materials played the dominant role in the manufacture of electronic devices, such as integrated logic circuits, nonvolatile memory, and so on. However, as the size of the devices scaled down ceaselessly from micrometers to below 10 nm, the traditional semiconductors have been hard to satisfy the requirement of enhanced specific capacitance, low gate leakage current, and high carrier mobility. Therefore, the exploration of new semiconductors as the device channels and the high-κ oxides as insulators becomes agog. Since the discovery of graphene, the successful fabrication of two-dimensional (2D) materials, especially the semiconductors with suitable band gap, has provided a promising way to overcome this drawback.

Among the 2D materials, molybdenum disulfide (MoS_2) with tunable properties based upon both layer count and the choice of substrate materials has drawn an increasing attention due to not only its good chemical stability and mechanical flexibility but also excellent optical and electrical properties [1, 2]. The energy band gap of the monolayer MoS_2 is about 1.80 eV while 1.20 eV for bulk. The promising performance of the electronic and optoelectronic devices made from MoS_2 layers, such as field-effect transistors [3–5], sensors [6], and photodetectors [7], proves it to be potential substitute of Si in conventional electronics and of organic semiconductors in wearable and flexible systems [8–11]. Even though single-layer MoS_2-based Field-effect transistors (FETs) have exhibited excellent performances with a high current on/off ratio about 10^8 and a low subthreshold swing ~ 77 mV/decade [3], its extensive applications were hindered by the synthesis of large area high-quality single-layer MoS_2 and the stability of the devices [12–14]. Multiple-layer MoS_2 could be more attractive due to the high density of states, which contributes to high drive current in the ballistic limit [15]. In addition, the carrier mobility of multilayer MoS_2 can be further improved significantly by high-κ oxides owing to the dielectric screening effects [16, 17]. Therefore, it is

* Correspondence: xkliu@szu.edu.cn; likuilong123@126.com
[1]College of Materials Science and Engineering, Shenzhen Key Laboratory of Micro-scale Optical Information Technology, Guangdong Research Center for Interfacial Engineering of Functional Materials, Shenzhen University, 3688 Nanhai Ave, Shenzhen 518060, People's Republic of China
[2]School of Electronic and Information Engineering (Department of Physics), Qilu University of Technology (Shandong Academy of Sciences), Jinan 250353, People's Republic of China
Full list of author information is available at the end of the article

essential and important to investigate the multilayer MoS_2/high-κ oxides heterojunctions.

In heterojunction electronic devices, the electron transport properties are precisely controlled by the energy band profiles at the interface between the semiconductor and insulator oxide in the terms of valence band offset (VBO) and conduction band offset (CBO). The VBO and CBO should be as large as possible to operate as a barrier in order to reduce the leakage current formed by the injection of holes and electrons, especially the CBO plays a pivotal role in the selection of suitable high-k oxides for a gate terminal and should be at least larger than 1 eV to avoid current leakage [18–20]. Meanwhile, the interface charges located at semiconductor/oxides impose an important effect on the band engineering and needs to be optimized through passivation technology, such as SiH_4 passivation, and CHF_3 treatment. In this paper, we investigated the band alignment of multilayer MoS_2/ ZrO_2 systems since the nature of the interface has a direct bearing on the characteristics of the devices, and the effect of CHF_3 plasma treatment on the band offset at MoS_2/ZrO_2 interface was explored.

Methods and Experiments

In the experiments, the multilayer MoS_2 films were grown on SiO_2/Si substrates by chemical vapor deposition (CVD) systems with MoO_3 and sulfur powder as the Mo sources and S precursors, respectively. During the growth process, Ar gas was used as the carrier gas and the growth temperature was 800 °C for 5 min. Then the MoS_2/ZrO_2 samples were prepared by transferring the large area multilayer MoS_2 film onto the ZrO_2/Si substrates using the poly methyl methacrylate (PMMA) method. The ZrO_2 oxide (15 nm) was deposited on Si at 200 °C using atomic layer deposition (BENEQ TFS-200) system with Tetrakis Dimethyl Amido Zirconium (TDMAZr) precursor as the zirconium source and water (H_2O) as the oxygen source. In order to investigate the effects of CHF_3 treatment on the band alignment at MoS_2/ZrO_2 interfaces, for one sample, the ZrO_2/Si substrate was treated by CHF_3 plasma with RF power about 20 W and flow rate about 26 sccm. Meanwhile, the plasma treatment time is about 60 s and the pressure was kept at 1 Pa during the process. Consequently, the resulted F dose is about 2.0×10^{14} atoms/cm^2 estimated by secondary ion mass spectrometry (SIMS) measurements. During the optimization process of the plasma treatment time, the CHF_3 plasma seriously deteriorated the material quality by introducing fluorine diffused into ZrO_2 largely when the time was set at 70 s. While when the plasma treatment time was 50 s, smaller than 60 s, SIMS results demonstrated no obvious F peak at the oxide surface. For the other sample, no CHF_3 plasma treatment was implemented. The Raman characteristics of the samples were taken in a RENISHAW system at room temperature. The X-ray photoelectron spectroscopy (XPS) was measured using a VG ESCALAB 220i-XL system. The photon energy of the monochromatized Al Kα x-ray source is about 1486.6 eV. During the measurements, the pass energy was set at 20 eV in order to obtain the XPS spectra. In addition, C 1 s peak (284.8 eV) was used to correct the core-level binding energy in order to eliminate the sample surface differential charging effect.

Results and Discussions

The Raman spectra of the as-grown and after-transferred multilayer MoS_2 were characterized at room temperature as shown in Fig. 1. Two prominent Raman modes labeled as $A_{1g}$and E^1_{2g} were observed in the spectrum. Specifically, E^1_{2g} mode is resulted from the opposite movement of in-plane S atoms with respect to the central Mo atom in the lower frequency region, whereas A_{1g} is relative to the out-of-plane vibrations of S atoms in the higher frequency region [21]. It has been observed that the E^1_{2g} and A_{1g} modes of MoS_2 undergo a red shift and blue shift, respectively, from monolayer to bulk samples, which is owing to the different interlayer Van der Waals restoring force and the influence of stacking-induced structure changes [21]. Therefore, the frequency difference (Δk) between the A_{1g} and E^1_{2g} modes is often used to evaluate the layer number or thickness of MoS_2 film. Herein, Δk of the grown MoS_2 film is about 25.32 cm^{-1}, indicating the film is more than six layers. In addition, the cross-sectional transmission electron microscopy (TEM) result displayed in the inset of Fig. 1 demonstrated the layer number of the grown MoS_2 was about 8 corresponding to the thickness about 4.5 nm. What is more, the Raman peak position and full width at half maximum (FWHM) of MoS_2 is almost the same

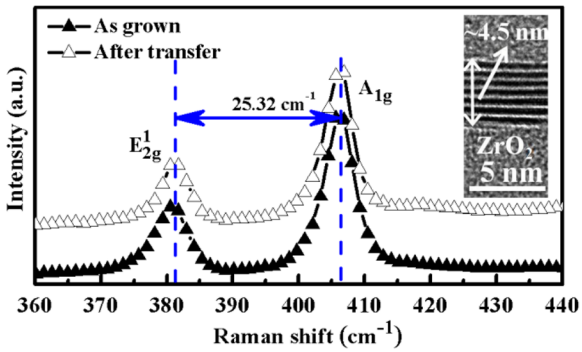

Fig. 1 The Raman spectroscopy of the ultrathin MoS_2 film before and after transfer. The inset is the cross-sectional transmission electron microscopy (TEM) image of the MoS_2 on ZrO_2/Si substrate, which shows the layers of MoS_2

before and after transfer, indicating that the transfer process exerts a small influence on the quality of the material.

XPS has been profoundly proved to be an efficient way to determine the band offset at the heterojunction interface [22, 23]. In MoS_2/ZrO_2 heterojunction, the VBO value was obtained from the change of the valence band spectra of the ZrO_2 between those of the bare oxide and with MoS_2 material [24]. Figure 2a, b showed the core level and valance band spectra of bare ZrO_2 and multilayer-MoS_2/ZrO_2, respectively. The intercept between the base line and the slope of the leading edge gives the valence band maximum (VBM) of the sample, where the Fermi level is taken as the reference level. The results demonstrated that the VBM of ZrO_2 and multilayer-MoS_2/ZrO_2 systems are about 1.88 eV and 0.06 eV, respectively. In addition, the Zr 3d core-level spectrum of bare ZrO_2 exhibits well-separated doublet peaks referred as Zr $3d_{5/2}$ and $3d_{3/2}$ with energy values of 182.05 eV and 184.45 eV, respectively, while the corresponding values for the MoS_2/ZrO_2 sample are 182.10 eV and 184.50 eV, respectively. The core-level change of Zr $3d_{5/2}$ or $3d_{3/2}$ ~ 0.05 eV is in the range of measurement and data processing error. In comparison with bare ZrO_2 sample, multilayer MoS_2 exerted little effects on the Zr 3d spectrum as shown in Fig. 2b. Then, the energy difference between the Zr $3d_{5/2}$ and VBM is 180.17 eV and 182.04 eV for the bare ZrO_2 sample and MoS_2/ZrO_2 sample, respectively. Consequently, the VBO value for the multilayer-MoS_2/ZrO_2 interface is about 1.87 ± 0.05 eV, mainly resulted from the VBM difference between the bare ZrO_2 and MoS_2/ZrO_2. Similarly, for the multilayer-MoS_2/ZrO_2 sample with CHF_3 plasma treatment before MoS_2 transfer, the VBM is about 0.02 eV as shown in Fig. 2c, almost identical to the sample without CHF_3 treatment. However, the Zr 3d spectrum moves toward higher energy by about 0.75 eV, Zr $3d_{5/2}$ ~ 182.85 eV, and $3d_{3/2}$~185.25 eV, indicating that the VBO value was enlarged by about 0.75 ± 0.04 eV after plasma etching. Then, the CBO value ΔE_C can be obtained according to the formula

$$\Delta E_C = E_{G,ZrO2} - E_{G,MoS2} - \Delta E_V. \quad (1)$$

where $E_{G,\ ZrO2}$ and $E_{G,\ MoS2}$ are the band gap of ZrO_2 and MoS_2, respectively, and ΔE_V corresponds to the VBO value. Normally, the band gap energy of oxide insulator can be obtained from the O 1 s loss energy spectrum [25]. Figure 3a shows the O 1 s loss energy spectrum of ZrO_2, and the $E_{G,\ ZrO2}$ is about 5.56 eV calculated from the energy difference by extrapolating the linear edge base line (535.95 eV) fit to the core level energy of Zr-O bonds (530.39 eV). The band gap of MoS_2 in this work is about 1.2 eV. Therefore, the CBO value for the sample without CHF_3 treatment is about 2.49 eV and 1.74 eV for the sample with CHF_3 treatment. Then, the schematic structures of the band engineering for the samples without and with CHF_3 plasma treatment are illustrated in Fig. 3b. Obviously, the multilayer-MoS_2/ZrO_2 system has a type I alignment, which facilitates electrons and holes confined in the MoS_2. Meanwhile, the large ΔE_C and ΔE_V for MoS_2/ZrO_2 interface implies that ZrO_2 could be a good gate dielectric for n- or p-channel multilayer MoS_2-based FETs application in term of gate leakage current suppression. In addition, the sample with plasma treatment has a higher VBO ΔE_V

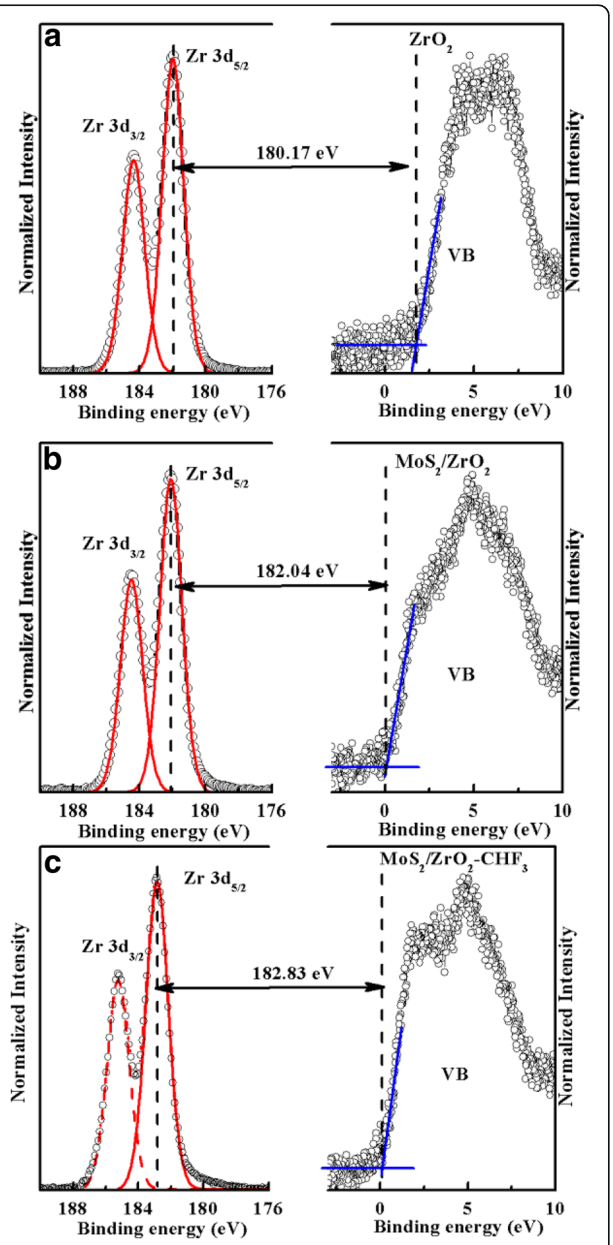

Fig. 2 The core-level Zr 3d and valence band spectra for **a** bare ZrO_2 oxide, **b** multilayer-MoS_2/ZrO_2 sample, and **c** CHF_3 plasma treated multilayer-MoS_2/ZrO_2 sample

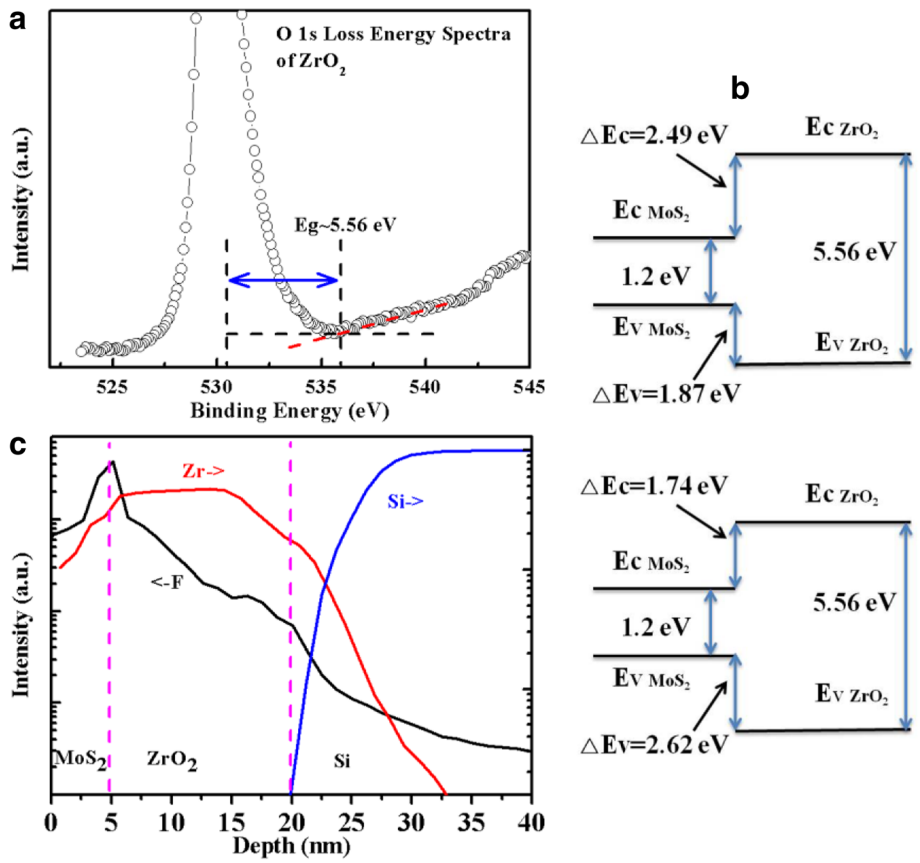

Fig. 3 **a** O 1 s photoelectron energy loss spectra for the ZrO_2 oxide. **b** The schematic structure of the energy band alignment at the MoS_2/ZrO_2 interface without (top) and with (bottom) CHF_3 plasma treatment. **c** The SIMS depth profiles (Si, Zr, and F) for the sample with CHF_3 plasma treatment

(lower CBO ΔE_C) in comparison with the sample without plasma treatment, which is better in the application of p-channel FETs.

The change of the band alignment at the multilayer MoS_2/ZrO_2 interface is believed to be closely related to the F-rich interfacial layer induced by the CHF_3 plasma treatment. Figure 3c displayed the SIMS result of the plasma-treated sample for Zr, F, and Si elements, presenting obvious F ions peak at the interface. Meanwhile, some F ions were diffused into the underlying ZrO_2 layer owing to its small size. At the MoS_2/ZrO_2 interface with CHF_3 plasma treatment, the enlargement of the VBO (reduction of the CBO) is mainly attributed to the up-shift of Zr 3d core-levels shown in Fig. 2c, indicating F ions have a strong interaction with Zr atoms. Then the effects of CHF_3 treatment on the electronic properties of the ZrO_2 oxide were investigated using Material Studio combined with the Cambridge Sequential Total Energy Package (CASTEP) based on density functional theory (DFT) [26]. The generalized gradient approximation for the exchange and correlation potential as proposed by Perdew-Burk-Ernzerhof (PBE) [27] was used to treat the ion-electron interactions together with the projector augmented wave potential (PAW) [28]. The plane wave cut-off energy is chosen to be 750 eV, and a Monkhorst–Pack k-mesh of $1 \times 1 \times 1$ is used to sample the Brillouin zone in the structure optimization and total energy calculation [29]. All the atoms were relaxed to their equilibrium positions until the total energy changes during the optimization finally converged to less than 10^{-6} eV/atom, the force and stress on each atom was converged to 0.003 eV/nm and 0.05 GPa, respectively, and the displacement was converged to 1×10^{-4} nm. Figure 4a, b shows the total and partial density of states (DOS) for both MoS_2/ZrO_2 samples, where zero eV corresponds to the Fermi level. Obviously, F ions have a strong interaction with Zr atoms, making part of the d-orbital from Zr atoms which is projected to valence band moves downward about 0.76 eV from – 0.06 to – 0.82 eV below the Fermi level, which is in consistent with the enlargement of the valance band offset $\Delta E_V \sim 0.75$ eV. F atoms tend to attract electrons owing to the large electronegativity (4.0) and become partially negatively charged and then further form dipoles with Zr atoms, eventually contribute to the change of the band offset. Therefore, the band change at the MoS_2/ZrO_2 interface introduced by

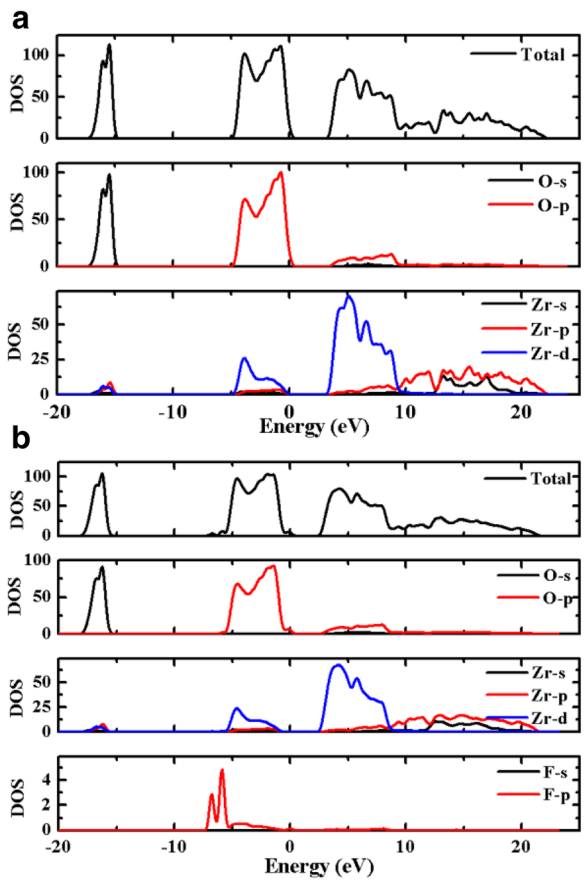

Fig. 4 The calculated total density of states (TDOS) and partial density of states (PDOS) for the samples without CHF_3 treatment (**a**) and with CHF_3 treatment (**b**)

the CHF_3 plasma treatment provides a promising way to adjust the band alignment at the heterojunctions, which facilitates the design of the related devices.

Conclusions

In this paper, we explored the energy band engineering at the multilayer MoS_2/ZrO_2 interface and investigated the effects of CHF_3 treatment using x-ray photoelectron spectroscopy. The results demonstrated that a type I alignment was formed at the MoS_2/ZrO_2 heterojunction interface with CBO and VBO about 2.49 eV and 1.87 eV, respectively. While the CHF_3 plasma treatment increases the VBO by about 0.75 ± 0.04 eV mainly due to the up-shift of Zr 3d core-level energy, which is consistent with the calculation results. This work proves the great potential applications of high-κ ZrO_2 oxide in multilayer MoS_2-based devices and provides a possible way to modify the interface energy band alignment.

Abbreviations

2D: Two-dimensional; CASTEP: Cambridge Sequential Total Energy Package; CBO: Conduction band offset; CVD: Chemical vapor deposition; DFT: Density functional theory; DOS: Density of states; FETs: Field-effect transistors; FWHM: Full width at half maximum; MoS_2: Molybdenum disulphide; PAW: Projector augmented wave; PBE: Perdew-Burk-Ernzerhof; PMMA: Poly methyl methacrylate; SIMS: Secondary ion mass spectrometry; TDMAZr: Tetrakis Dimethyl Amido Zirconium; TEM: Transmission electron microscopy; TMDs: Transition metal dichalcogenides; VBO: Valence band offset; XPS: X-ray photoelectron spectroscopy; ZrO_2: Zirconium dioxide

Acknowledgements

We thank the reviewers for their valuable comments, and the Photonics Center of Shenzhen University for technical support.

Funding

The National Key Research and Development Program of China (2017YFB0404100), the National Natural Science Foundation of China (61504083,61804086), the PhD Start-up Fund of Natural Science Foundation of Guangdong Province (2017A030310424), the Science and Technology Foundation of Shenzhen (JCYJ20160226192033020), the National Taipei University of Technology-Shenzhen University Joint Research Program (2018001), and the Natural Science Foundation of Shandong Province (Grant No. ZR2017LF022, ZR2016AM25) act as guide to the design of the study and the collection, analysis, and interpretation of the data and the publication of the study.

Availability of data and materials

All data generated or analyzed during this study are included in this published article.

Authors' contributions

CH, KLL, WJW, ZWL, and QL carried out the related experiments and data analysis. KLL drafted the manuscript. XKL supervised the experiments and the writing of the manuscript. JPA, WH, JW, WJY, and RJC provided suggestions and guidance for the experiments and data analysis. ZWL and WM carried out the calculation. All authors read and approved the final manuscript.

Authors' information

XKL is an associate professor in materials physics. CH and ZWL are students in material growth and calculation. KLL and WJW are associate professors in material characterization and analysis. JPA, JW, WH, WJY, and RJC are professors in materials science. WM is an associate professor in calculation and analysis. QL is assistant research in material growth and characterization.

Competing interests

The authors declare that they have no competing interests.

Publisher's Note

Author details

[1]College of Materials Science and Engineering, Shenzhen Key Laboratory of Micro-scale Optical Information Technology, Guangdong Research Center for Interfacial Engineering of Functional Materials, Shenzhen University, 3688 Nanhai Ave, Shenzhen 518060, People's Republic of China. [2]School of Electronic and Information Engineering (Department of Physics), Qilu University of Technology (Shandong Academy of Sciences), Jinan 250353, People's Republic of China. [3]Institute of Materials research and Engineering (IMRE), 2 Fusionopolis Way, Innovis, #08-03, Singapore 138634, Singapore. [4]College of Electronic Science and Technology, Shenzhen University, Shenzhen 518060, People's Republic of China. [5]The Institute of Engineering Innovation, School of Engineering, The University of Tokyo, Tokyo 113-0032, Japan. [6]State Key Laboratory of Functional Materials for Informatics, Shanghai Institute of Microsystem and Information Technology, CAS, Shanghai 200050, People's Republic of China. [7]Department of Chemical Engineering and Biotechnology, National Taipei University of Technology (Taipei Tech), 10608 Taipei, Taiwan.

Received: 5 October 2018 Accepted: 5 December 2018
Published online: 17 December 2018

References

1. Chhowalla M, Shin HS, Eda G, Li L-J, Loh KP, Zhang H (2013) The chemistry of two-dimensional layered transition metal dichalcogenide nanosheets. Nat Chem 5:263
2. Huang X, Zeng Z, Zhang H (2013) Metal dichalcogenide nanosheets: preparation, properties and applications. Chem Soc Rev 42:1934–1946
3. Radisavljevic B, Radenovic A, Brivio J, Giacometti V, Kis A (2011) Single-layer MoS_2 transistors. Nat Nanotechnol 6:147
4. Wang H, Yu L, Lee Y-H, Shi Y, Hsu A, Chin ML, Li L-J, Dubey M, Kong J, Palacios T (2012) Integrated circuits based on bilayer MoS_2 transistors. Nano Lett 12:4674–4680
5. Pu J, Yomogida Y, Liu K-K, Li L-J, Iwasa Y, Takenobu T (2012) Highly flexible MoS_2 thin-film transistors with ion gel dielectrics. Nano Lett 12:4013–4017
6. Perkins FK, Friedman AL, Cobas E, Campbell PM, Jernigan GG, Jonker BT (2013) Chemical vapor sensing with monolayer MoS_2. Nano Lett 13:668–673
7. Yin Z, Li H, Li H, Jiang L, Shi Y, Sun Y, Lu G, Zhang Q, Chen X, Zhang H (2012) Single-layer MoS_2 phototransistors. ACS Nano 6:74–80
8. Roy K, Padmanabhan M, Goswami S, Sai TP, Ramalingam G, Raghavan S, Ghosh A (2013) Graphene–MoS_2 hybrid structures for multifunctional photoresponsive memory devices. Nat Nanotechnol 8:826
9. Schmidt H, Wang S, Chu L, Toh M, Kumar R, Zhao W, Castro Neto AH, Martin J, Adam S, Özyilmaz B, Eda G (2014) Transport properties of monolayer MoS_2 grown by chemical vapor deposition. Nano Lett 14: 1909–1913
10. Yu L, Lee Y-H, Ling X, Santos EJG, Shin YC, Lin Y, Dubey M, Kaxiras E, Kong J, Wang H, Palacios T (2014) Graphene/MoS_2 hybrid technology for large-scale two-dimensional electronics. Nano Lett 14:3055–3063
11. Lee G-H, Yu Y-J, Cui X, Petrone N, Lee C-H, Choi MS, Lee D-Y, Lee C, Yoo WJ, Watanabe K, Taniguchi T, Nuckolls C, Kim P, Hone J (2013) Flexible and transparent MoS_2 field-effect transistors on hexagonal boron nitride-graphene heterostructures. ACS Nano 7:7931–7936
12. Yu Y, Li C, Liu Y, Su L, Zhang Y, Cao L (2013) Controlled scalable synthesis of uniform, high-quality monolayer and few-layer MoS_2 films. Sci Rep 3:1866
13. Li H, Yin Z, He Q, Li H, Huang X, Lu G, Fam DWH, Tok AIY, Zhang Q, Zhang H (2012) Fabrication of single-and multilayer MoS_2 film-based field-effect transistors for sensing NO at room temperature. Small 8:63–67
14. Lee YH, Zhang XQ, Zhang W, Chang MT, Lin CT, Chang KD, Yu YC, Wang JTW, Chang CS, Li LJ, Lin TW (2012) Synthesis of large-area MoS_2 atomic layers with chemical vapor deposition. Adv Mater 24:2320–2325
15. Kim S, Konar A, Hwang W-S, Lee JH, Lee J, Yang J, Jung C, Kim H, Yoo J-B, Choi J-Y, Jin YW, Lee SY, Jena D, Choi W, Kim K (2012) High-mobility and low-power thin-film transistors based on multilayer MoS_2 crystals. Nat Commun 3:1011
16. Laskar MR, Ma L, Kannappan S, Park PS, Krishnamoorthy S, Nath DN, Lu W, Wu Y, Rajan S (2013) Large area single crystal (0001) oriented MoS_2. Appl Phys Lett 102:252108
17. Liu H, Xu K, Zhang X, Ye PD (2012) The integration of high-k dielectric on two-dimensional crystals by atomic layer deposition. Appl Phys Lett 100:152115
18. Tao J, Chai JW, Zhang Z, Pan JS, Wang SJ (2014) The energy-band alignment at molybdenum disulphide and high-k dielectrics interfaces. Appl Phys Lett 104:232110
19. Afanas'ev VV, Chiappe D, Huyghebaert C, Radu I, De Gendt S, Houssa M, Stesmans A (2015) Band alignment at interfaces of few-monolayer MoS_2 with SiO2 and HfO2. Microelectron Eng 147:294–297
20. Wang SJ, Huan ACH, Foo YL, Chai JW, Pan JS, Li Q, Dong YF, Feng YP, Ong CK (2004) Energy-band alignments at ZrO_2 / Si, SiGe, and Ge interfaces. Appl Phys Lett 85:4418–4420
21. Lee C, Yan H, Brus LE, Heinz TF, Hone J, Ryu S (2010) Anomalous lattice vibrations of single- and few-layer MoS_2. ACS Nano 4:2695–2700
22. Kraut EA (1984) Heterojunction band off-sets: variation with ionization potential compared to experiment. Journal of Vacuum Science & Technology B: Microelectronics Processing and Phenomena 2:486–490
23. Tuan AC, Kaspar TC, Droubay T, JWR J, Chambers SA (2003) Band offsets for the epitaxial TiO_2/$SrTiO_3$/Si(001) system. Appl Phys Lett 83:3734–3736
24. Pradhan SK, Xiao B, Pradhan AK (2016) Energy band alignment of high-k oxide heterostructures at MoS_2/Al_2O_3 and MoS_2/ZrO_2 interfaces. J Appl Phys 120:125305
25. Miyazaki S (2001) Photoemission study of energy-band alignments and gap-state density distributions for high-k gate dielectrics. Journal of Vacuum Science & Technology B: Microelectronics and Nanometer Structures Processing, Measurement, and Phenomena 19:2212–2216
26. Segall MD, Philip JDL, Probert MJ, Pickard CJ, Hasnip PJ, Clark SJ, Payne MC (2002) First-principles simulation: ideas, illustrations and the CASTEP code. J Phys Condens Matter 14:2717
27. Perdew JP, Burke K, Ernzerhof M (1996) Generalized gradient approximation made simple. Phys Rev Lett 77:3865–3868
28. Blöchl PE (1994) Projector augmented-wave method. Phys Rev B 50: 17953–17979
29. Monkhorst HJ, Pack JD (1976) Special points for Brillouin-zone integrations. Phys Rev B 13:5188–5192